

Total flavonoids of *Rhizoma Drynariae* combined with calcium attenuate osteoporosis by reducing reactive oxygen species generation

PANYUN MU^{1*}, YIMEI HU^{1*}, XU MA¹, JINGRU SHI², ZHENDONG ZHONG³ and LINGYUAN HUANG⁴

¹Department of Orthopedics, Hospital of Chengdu University of Traditional Chinese Medicine, Chengdu, Sichuan 610075;

²Department of Orthopedics, Hospital of Chengdu University of Traditional Chinese Medicine, Chengdu, Sichuan 611137;

³Laboratory Animal Research Institute of Sichuan Provincial People's Hospital, Chengdu, Sichuan 610072;

⁴Chengdu Lilai Biotechnology Co., Ltd., Chengdu, Sichuan 610041, P.R. China

Received January 7, 2020; Accepted February 1, 2021

DOI: 10.3892/etm.2021.10050

Abstract. In the present study, the effects of total flavonoids of *Rhizoma Drynariae* (TFRD) and calcium carbonate (CaCO₃) on osteoporosis (OP) were assessed in a rat model of OP. For this purpose, 36 Sprague-Dawley rats, aged 3 months, were randomly divided into a group undergoing sham surgery (sham-operated group), model group (OP group), CaCO₃ group (OP + CaCO₃ group), TFRD group (OP + TFRD group), TFRD combined with CaCO₃ group (OP + TFRD + CaCO₃ group) and TFRD and CaCO₃ combined with N-acetyl cysteine group (OP + TFRD + CaCO₃ + NAC group). The rat model of OP was established by bilateral ovariectomy. The changes in bone mineral density (BMD), bone volume parameters and bone histopathology in the rats from each group were observed. The levels of serum reactive oxygen species, superoxide dismutase (SOD), malondialdehyde, glutathione peroxidase (GSH-Px), interleukin (IL)-6, IL-1 β , TNF- α , and the levels of bone tissue runt-related transcription factor 2 (RUNX2), osteoprotegerin (OPG), osteocalcin (BGP), PI3K, p-PI3K, AKT, p-AKT, mammalian target of rapamycin (mTOR) and p-mTOR were measured in the rats of each group. The induction of OP was associated with a marked decrease in BMD, bone mineral content, bone volume fraction and trabecular thickness, and decreased serum levels of SOD and GSH-Px. Moreover, the expressions of RUNX2, OPG, BGP were downregulated and an upregulation of p-PI3K, p-AKT and p-mTOR were observed

in osteoporotic rats. However, treatment with TFRD and CaCO₃ restored all the aforementioned parameters to almost normal values. Furthermore, the findings on histopathological evaluation were consistent with the biochemical observations. Taken together, the findings of the present study demonstrated that TFRD and CaCO₃ significantly increased the antioxidant capacity in rats with OP, increased BMD and reduced bone mineral loss, and may be useful for the prevention and treatment of OP.

Introduction

Osteoporosis(OP) is a systemic bone metabolic disorder, which is characterized by decreased bone density and degeneration of the bone microstructure, resulting in increased bone brittleness and risk of fractures (1). Bone modeling and remodeling are dynamic metabolic processes that are mainly regulated by two types of bone cells: Osteoblasts, which secrete bone matrix and accelerate calcium deposition; and osteoclasts, which dissolve mineralized bone matrix (2); the imbalance between these two processes leads to the development of OP. Along with an increase in age, the absorption of calcium in the body decreases with the reduction of osteoblast production, whereas endocrine and metabolic factors also play a crucial role in reducing the bioavailability of calcium (3). At present, due to the aging of the population, the incidence of OP among the elderly is increasing annually. Research by several patient investigation centers in China in 2014 indicated that the prevalence of OP in individuals aged 50-59 years was 15.5%, and its prevalence in individuals aged 80-89 years was 81% (4). Furthermore, among patients with OP aged between 50 and 89 years, the spine accounts for 28% of the total morbidity, the femur accounts for 15%, and both the spine and femur account for 31% (5). With an increasing incidence of OP, the social burden has greatly increased.

It has been demonstrated that oxidative stress is associated with the pathogenesis of OP, and the pathogenesis of OP is accompanied by an increase in oxidative stress and apoptosis (6). Accumulating evidence has indicated that reactive oxygen species (ROS)-induced oxidative stress increases with aging,

Correspondence to: Dr Yimei Hu, Department of Orthopedics, Hospital of Chengdu University of Traditional Chinese Medicine, 39 Twelve Bridge Road, Jinniu, Chengdu, Sichuan 610075, P.R. China
E-mail: huyimei66@163.com

*Contributed equally

Key words: osteoporosis, total flavonoids of *Rhizoma Drynariae*, oxidative stress

which is related to the pathophysiology of postmenopausal OP (7). An excess of ROS can inhibit osteoblast differentiation and proliferation, enhance osteoclastic differentiation, and ultimately lead to greater bone reabsorption (8). Dietary supplementation with antioxidants is an effective approach to improving the damage caused by excessive ROS generation. N-acetyl cysteine (NAC) is one of the most widely used antioxidants in the context of clinical studies, animal and cell culture experiments (9). A number of conclusions have been based on the outcome of experiments using NAC. When treatment with NAC was found to inhibit a particular cellular process or response, it was typically concluded that ROS play an active role in this process. For example, the stimulating effects of gonadectomy on oxidative stress, osteoblast apoptosis and osteoclastogenesis, and the loss of bone mass, were shown to be reduced by supplementation with antioxidants, such as NAC and ascorbate (10,11). Amongst several other applications, NAC has also been used to investigate the physiological roles of mitochondrial ROS (12,13). Additionally, Yamada *et al.* (14) demonstrated that NAC markedly promoted the differentiation of osteoblastic cells and accelerated bone regeneration. Calcium ion is an essential structural component of the skeleton, and oxidative stress is an important mediator of bone loss (15). The administration of antioxidants may protect bones from OP and may also help accelerate the healing of fractured bones.

Under conditions of oxidative stress, phosphoinositide 3-kinase (PI3K)/protein kinase B (AKT) is a vital signaling pathway that participates in regulating the proliferation, death and survival of cells, and serves as a targeted pathway of intervention treatment (16). Studies on the PI3K signaling pathway have reported that AKT and its related downstream signaling molecules are key factors for regulating endochondral ossification (17,18). AKT may affect bone formation and osteoblast survival by maintaining the class O forkhead box transcription factors (FOXOs) in the cytoplasm (19). These previous studies have indicated that the PI3K/AKT signaling pathway is closely associated with the occurrence of OP.

The present study investigated the use of total flavonoids of *Rhizoma Drynariae* (TFRD) and calcium in the treatment of OP. TFRD are considered to be natural antioxidant agents and free radical scavengers, and may help prevent bone loss; the intake of calcium can attenuate bone loss and improve bone mineralization (20). Therefore, it was hypothesized that TFRD combined with calcium could improve OP through relieving oxidative stress. For this purpose, in the present study, an OP model was established by ovariectomy in female rats, and the effects of the combined use of TFRD and calcium carbonate (CaCO₃) on bone mineral density (BMD), bone mineral content (BMC) and oxidative stress were determined. The findings of the present study may provide a basis for the future clinical prevention and treatment of OP.

Materials and methods

Experimental animals. A total of 36 female specific pathogen-free (SPF) Sprague-Dawley rats, aged 3 months and weighing 230±20 g, were purchased from Chengdu Dashuo Experimental Animal Co., Ltd. (license no. SYXK 2018-119). The rats were kept in cages with a controlled environment

(temperature 24°C and humidity 40%) and a 12/12-h light/dark cycle and were provided with free access to food and water. The present study was approved by the Animal Care Unit and Use Committee of Chengdu University of TCM (no. 20190078).

Experimental reagents. CaCO₃, TFRD (Guangzhou Baozhilin Pharmacy), NAC (Sigma-Aldrich; Merck KGaA) and kits for superoxide dismutase (SOD; cat. no. A001-3-2), malondialdehyde (MDA; cat. no. A003-1-2), ROS (cat. no. E004-1-1) and glutathione peroxidase (GSH-Px; cat. no. A005-1-2) were purchased from Nanjing Jiancheng Bioengineering Institute; kits for IL-6 (cat. no. ZC-36404), IL-1β (cat. no. ZC-M6681), TNF-α (cat. no. ZC-37624) were purchased from ZCIBIO Technology Co., Ltd.; kits for hematoxylin and eosin (H&E; cat. no. C0105S) staining were purchased from Beyotime Institute of Biotechnology; kits for Masson's staining (cat. no. 60532ES58) were purchased from Shanghai Maikun Chemical Co., Ltd.; kits for protein extraction (cat. no. P1202) and SDS-PAGE gel preparation (cat. no. PG112) were purchased from Shanghai Epizyme Biotech; RIPA buffer reagent (cat. no. P0013) and kit for BCA (cat. no. P0009) were purchased from Beyotime Institute of Biotechnology; primary antibodies against runt-related transcription factor 2 (RUNX2; cat. no. sc-390351), osteoprotegerin (OPG; cat. no. sc-390518), osteocalcin (BGP; cat. no. sc-365797), AKT (cat. no. sc-5298), p-AKT (cat. no. sc-377556), mammalian target of rapamycin (mTOR; cat. no. sc-517464), p-mTOR (cat. no. sc-293133), PI3K (cat. no. sc-365290) and p-PI3K (cat. no. sc-1637) were purchased from Santa Cruz Biotechnology, Inc. Horseradish peroxidase-labeled goat anti-rabbit secondary antibody (cat. no. #56970) was purchased from Cell Signaling Technology, Inc. kit for Enhanced chemiluminescence (ECL; cat. no. KF001) was purchased from Affinity Biosciences.

Experimental instruments. The Dual Energy X-Ray Bone Densitometer (Hologic, Inc.) continuous-wavelength multi-functional microplate reader (Tecan Group, Ltd.) and the BA200 Digital trinocular micro-camera system (McAudi Industry Group) and the 5200 Quantity One gel imaging software (Tanon Science and Technology Co., Ltd.) were used in the present study.

Rat model of ovariectomy-induced OP. A total of 36 senile female SPF rats were adaptively fed for 1 week, and then randomly divided into 6 groups (n=6 per group) as follows: Non-ovariectomy control group (sham-operated group), model group (OP group), TFRD group (OP + TFRD group), CaCO₃ group (OP + CaCO₃ group), TFRD combined with CaCO₃ group (OP + TFRD + CaCO₃ group) and TFRD and CaCO₃ combined with NAC group (OP + TFRD + CaCO₃ + NAC group). Following anesthesia with 35 mg/kg pentobarbital sodium (intraperitoneal), the rats in the sham-operated group underwent sham surgery to remove 1 g of adipose tissue around the ovary, and the rats of the other 5 groups underwent bilateral ovariectomy. At 4 weeks post-surgery (from the 5th week onwards), the rats of the respective groups were intragastrically given CaCO₃ (20 mg/kg/day), TFRD (50 mg/kg/day) or TFRD (50 mg/kg/day) and CaCO₃ (20 mg/kg/day). The rats in the OP + TFRD + CaCO₃ + NAC group were intraperitoneally injected with 500 mg/kg/day

NAC, and TFRD (50 mg/kg/day) + CaCO₃ (20 mg/kg/day) were administered via intragastric administration once a day. The rats in the sham-operated and model (OP) groups were administered 0.9% normal saline intragastrically once daily for 10 consecutive weeks. NAC was injected once every 2 weeks for a total of 5 times. The dosage of TFRD and CaCO₃ was selected based on the research reports of Fang *et al* (21) and Zhu *et al* (22).

Sample collection. After treatment for 10 weeks, blood samples were collected from the abdominal aorta. For blood collection, 35 mg/kg pentobarbital sodium was injected into the abdominal cavity to anesthetize the rats. After successful anesthesia, the rats were transferred to a pre-sterilized super-clean worktable, an incision was performed along the middle of the abdomen, and then the left abdominal wall was cut laterally, fully exposing the abdominal organs, carefully exposing the retroperitoneum and the abdominal aorta. Then, the needle of a 10-ml syringe was injected through the blood vessel wall at an angle of 30 degrees with the needle eye facing down, the direction was then changed to horizontal, and 5-10 ml blood was drawn from each rat. The rats were sacrificed by exsanguination after blood collection. Next, the hip joint was exposed by routine peeling with a sterilized scalpel and scissors under aseptic conditions. The joint capsule was cut open, the round ligament of the femoral head was severed above the femoral head, and the bilateral femoral heads were removed. The left femur tissue of each rat was fixed in 4% paraformaldehyde fixation solution for 24h, and then decalcified with 15% EDTA-2Na for 4 weeks. After decalcification, the intact femur was embedded in paraffin, cut into sections (3-5 μ m), and the sections were subjected to H&E and Masson's staining. The left proximal femur was quickly frozen in liquid nitrogen for western blotting detection. The intact right femur was stored at 4°C in tissue fixation solution for follow-up dual energy X-Ray bone densitometry.

Dual-energy X-Ray bone density measurement. Dual-energy X-ray bone densitometry uses X-rays to examine the bones of the body and processes the corresponding data through a special chip microcomputer system. It can provide accurate measurement and positioning data, and the detection speed is high. Therefore, the bone morphometric parameters of the femurs were determined using a dual-energy X-ray bone densitometer. The femurs of the rats were resected and the attached cartilage tissue was removed. The dual-energy X-ray bone densitometer and its accompanying small animal cascade standard analysis software (Hologic discovery Wi; Hologic, Inc.) were then immediately used to determine the BMD (g/cm²) and BMC (g/cm²).

H&E and Masson's staining. Bone tissue from each group of rats was decalcified in 15% EDTA-2Na solution. Then cleaned using xylene and embedded in melted paraffin. The paraffin block was then cut into 3-5- μ m sections using a microtome. Finally, the sections were dewaxed and at 50°C subjected to H&E (hematoxylin staining for 10-20 min in warm water and eosin staining for 3-5 min at 50°C) and Masson's trichrome staining (celestine blue staining for 2-3 min, followed by hematoxylin staining for 2-3 min, Ponceau masson acid

fuchsin staining for 10min and aniline blue staining for 5 min; all performed at 37°C). The BA200 Digital trinocular micro-camera system was then used to capture images of the sections. Bone structure parameters, including bone volume over tissue volume (bone volume fraction; BV/TV, %) and trabecular thickness (Tb.Th, mm) were then analyzed using the VIDAS automated image analysis system (Zeiss AG).

Detection of serum indices. After treatment for 10 weeks, blood (5-10 ml) was extracted from the abdominal aorta as mentioned above and centrifuged at 2,030 x g at 4°C for 10 min. The serum was separated and cryopreserved at -80°C. The serum levels of IL-6, IL-1 β , TNF- α , SOD, ROS, MDA and GSH-Px were determined by sequential sample loading according to the instructions of the manufacturer of the respective kits. The content of IL-6 in each group was measured at 450 nm using a continuous-wavelength multifunctional enzyme analyzer. The content of IL-1 β in each group was determined at 570 nm, the content of TNF- α in each group was measured at 492 nm, the content of SOD in each group was detected at 550 nm, the content of MDA in each group was determined at 532 nm, the content of GSH-Px in each group was detected at 412 nm, and the content of ROS in each group was determined at 485 nm. Three test repetitions were performed for each indicator.

Western blot analysis. For the determination of protein expression levels, total protein was collected using RIPA buffer reagent, protein concentration was determined using a BCA kit. Then, a total of 40 μ g protein were loaded per lane and separated by 10% SDS-PAGE and transferred onto PVDF membranes. Membranes were then blocked with 5% skimmed milk powder at room temperature for 2 h. The membranes were blotted with primary antibodies against RUNX2, OPG, BGP PI3K, p-PI3K, AKT, p-AKT, mTOR and p-mTOR (all, 1:1,000) at 4°C overnight; β -actin (1:10,000) was used as a loading control. The membranes were washed 3 times with 0.1% TBST buffer for 10 min each time, followed by incubation at room temperature for 2-3 h with the secondary antibody (1:5,000). The protein bands resulting from Western blot analysis were visualized by ECL. The A-value of the target band was analyzed using Quantity One gel imaging software, and the ratio of the A-value of the target band to the β -actin band was considered as the relative expression of the target protein; the blots were performed in triplicate.

Statistical analysis. The data were statistically analyzed using SPSS 20.0 software (IBM Corp.). After verification of a normal or non-normal distribution by the Shapiro-Wilk test, two-tailed Student's t-test and one-way ANOVA followed by Tukey's post-hoc test was performed to analyze the variables of normal distribution. When data were non-normally distributed, log-transformation was applied. For all the analyses, P<0.05 was considered to indicate a statistically significant difference.

Results

Effects of TFRD combined with CaCO₃ on the femur microstructure of OP rats. Compared with the sham-operated group, the BMD, BMC, BV/TV and Tb.Th were markedly

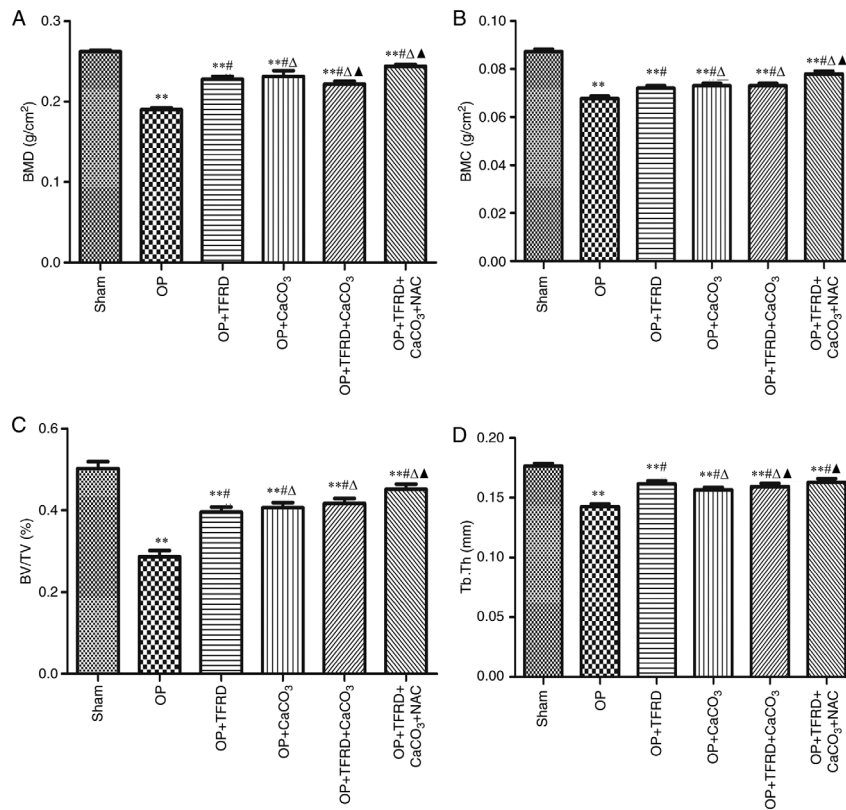


Figure 1. Comparisons of femur microstructure between the rats in the different groups. (A) BMD; (B) BMC; (C) BV/TV; and (D) Tb.Th. The data are expressed as mean \pm SD. Compared with the sham-operated group, ** $P<0.01$; compared with the OP group, # $P<0.05$; compared with the OP + TFRD group, $\Delta P<0.05$; compared with the OP + CaCO₃ group, $\blacktriangle P<0.05$. OP, osteoporosis; TFRD, total flavonoids of Rhizoma Drynariae; CaCO₃, calcium carbonate; NAC, N-acetylcysteine; BMD, bone mineral density; BMC, bone mineral content; BV/TV, bone volume fraction; Tb.Th, trabecular thickness.

decreased in the OP, OP + TFRD, OP + CaCO₃, OP + TFRD + CaCO₃ and OP + TFRD + CaCO₃ + NAC groups ($P<0.05$; Fig.1 A-D); compared with the OP group, the BMD, BMC, BV/TV and Tb.Th were markedly increased in the OP + TFRD, OP + CaCO₃, OP + TFRD + CaCO₃ and OP + TFRD + CaCO₃ + NAC groups ($P<0.05$; Fig. 1A-D); compared with the OP + TFRD and OP + CaCO₃ groups, BMD, BMC and BV/TV were markedly elevated in the rats in the OP + TFRD + CaCO₃ + NAC group ($P<0.05$; Fig. 1A-D). These results indicated that TFRD, CaCO₃ and NAC markedly ameliorated bone density in OP rats.

Effects of TFRD combined with CaCO₃ on the pathological changes of bone in OP rats. Compared with the sham-operated group, in the OP model rats, the osteolysis of the femur, bone trabeculae were disconnected, and there was a large number of bone marrow cells in the bone marrow cavity; blood cells, macrophages, adipocytes or mesenchymal cells at different developmental stages were also observed. Compared with the OP, OP + TFRD and OP + CaCO₃ groups, the structure of the bone tissue was clear, complete and continuous, and the bone trabeculae exhibited a uniform thickness in the OP + TFRD + CaCO₃ + NAC group (Fig. 2A). Compared with the sham-operated group, in the OP model rats, osteogenic tissue fractures were observed in some regions, the trabecular bone was markedly reduced, and the trabeculae were fine and evidently disconnected. Compared with the OP, OP + TFRD and OP + CaCO₃ groups, the structure of the bone tissue

was complete and clear, and a small number of small cracks were observed in some bone trabeculae in the OP + TFRD + CaCO₃ + NAC group (Fig. 2B). These results indicated that TFRD, CaCO₃ and NAC supplementation promoted the pathological improvement of bone tissue in OP rats.

Effects of TFRD combined with CaCO₃ on the expression of bone formation-related genes in OP rats. Compared with the sham-operated group, the protein expression of RUNX2 was significantly decreased in rats in the OP and OP + CaCO₃ groups ($P<0.01$ and $P<0.05$, respectively; Fig. 3A); the expression of OPG in the rats in the OP, OP + TFRD and OP + CaCO₃ groups was significantly decreased ($P<0.01$, $P<0.05$ and $P<0.01$, respectively; Fig. 3A); and the expression of BGP in the rats in the OP group was markedly decreased ($P<0.01$; Fig. 3A). Compared with the OP group, the protein expression of RUNX2 and BGP were markedly increased in the rats in the OP + TFRD + CaCO₃ and OP + TFRD + CaCO₃ + NAC groups ($P<0.05$, $P<0.05$, $P<0.05$ and $P<0.01$, respectively; Fig. 3A); the protein expression of OPG was significantly increased in rats of the OP + TFRD, OP + TFRD + CaCO₃ and OP + TFRD + CaCO₃ + NAC groups ($P<0.05$, $P<0.05$ and $P<0.01$; Fig. 3A). These results suggested that TFRD, CaCO₃ and NAC supplementation increased the expression levels of bone formation-related genes in OP rats.

Effects of TFRD combined with CaCO₃ on inflammation and oxidative stress in OP rats. Compared with the sham-operated

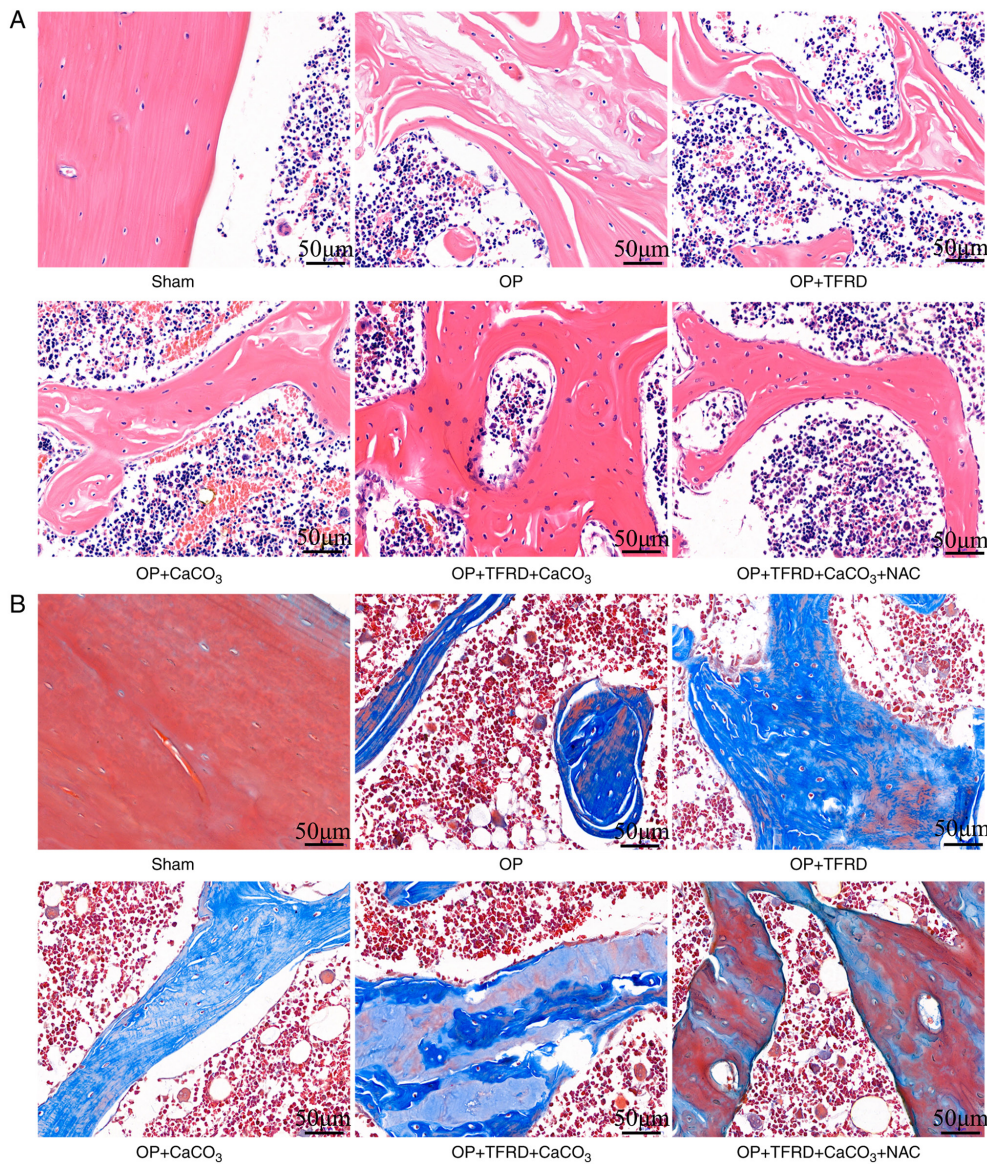


Figure 2. Analysis of bone histopathology by H&E and Masson's trichrome staining. Representative microscopic images of decalcified distal bone tissue paraffin sections stained with (A) H&E and (B) Masson's trichrome stain (magnification, $\times 400$; scale bar, $50\ \mu\text{m}$). H&E, hematoxylin and eosin; OP, osteoporosis; TFRD, total flavonoids of *Rhizoma Drynariae*; CaCO_3 , calcium carbonate; NAC, N-acetylcysteine.

group, the levels of IL-6 and IL-1 β were significantly increased in rats of the OP, OP + TFRD and OP + CaCO_3 groups (all $P < 0.05$; Fig. 4A and B), the levels of TNF- α , ROS and MDA were significantly increased in rats of the OP and OP + TFRD groups (all $P < 0.05$; Fig. 4C-E), whereas SOD and GSH-Px activity was significantly decreased in rats of the OP, OP + TFRD, OP + CaCO_3 and OP + TFRD + CaCO_3 groups (all $P < 0.05$; Fig. 4F and G). Compared with the OP group, the levels of IL-6 and TNF- α were significantly decreased in rats of the OP + TFRD + CaCO_3 and OP + TFRD + CaCO_3 + NAC groups, the levels of IL-1 β , ROS and MDA were markedly decreased in rats of the OP + TFRD + CaCO_3 + NAC group, and SOD and GSH-Px activity was significantly increased in rats of the OP + TFRD + CaCO_3 + NAC group (all $P < 0.05$; Fig. 4A-G). Compared with the OP + TFRD group, the levels of ROS and MDA were markedly decreased in rats of the OP + TFRD + CaCO_3 + NAC group ($P < 0.05$; Fig. 4D-E). These results revealed that OP increased the levels of oxidative

stress-related markers in the serum, whereas TFRD, CaCO_3 and NAC supplementation reduce oxidative stress in OP rats.

Effects of TFRD combined with CaCO_3 on the oxidative stress pathway in OP rats. Compared with the sham-operated group, the contents of AKT, p-AKT, mTOR, p-mTOR and PI3K exhibited no significant differences in the other groups ($P > 0.05$; Fig. 5A). The content of p-PI3K was significantly increased in rats of the OP group ($P < 0.01$; Fig. 5A). Compared with the OP group, the content of p-PI3K in the OP + TFRD + CaCO_3 and OP + TFRD + CaCO_3 + NAC groups was significantly decreased (all $P < 0.01$; Fig. 5A). Compared with the sham-operated group, the p-AKT/AKT ratio was markedly increased in OP rats ($P < 0.01$), the p-mTOR/mTOR ratio was significantly increased in the OP, OP + TFRD and OP + CaCO_3 groups ($P < 0.01$, $P < 0.05$ and $P < 0.01$, respectively), and the p-PI3K/PI3K ratio was markedly increased in rats of the OP, OP + TFRD, OP + CaCO_3 and OP + TFRD + CaCO_3 groups ($P < 0.01$,

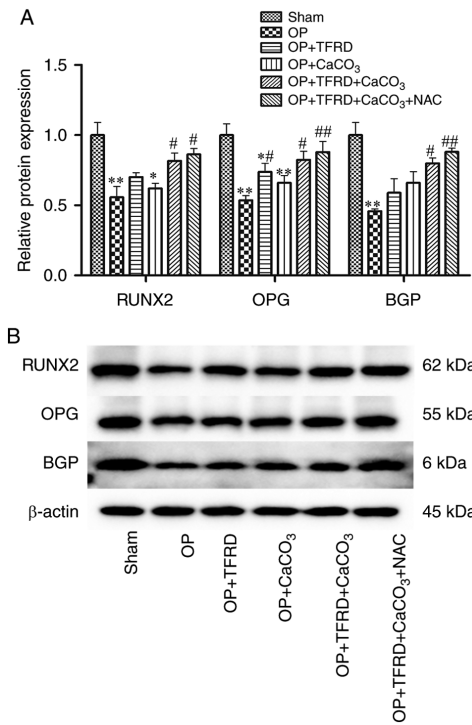


Figure 3. Western blot analysis of the expression of bone formation-related proteins in OP rats. (A) Relative expression of RUNX2, OPG and BGP; (B) protein band density was calculated as a ratio relative to β-actin protein levels. The data are expressed as the mean ± SD. Compared with the sham-operated group, *P<0.05 and **P<0.01; compared with the OP group, #P<0.05 and ##P<0.01; RUNX2, Runt-related transcription factor 2; OPG, osteoprotegerin; BGP, osteocalcin; OP, osteoporosis; TFRD, total flavonoids of *Rhizoma Drynariae*; CaCO₃, calcium carbonate; NAC, N-acetyl cysteine.

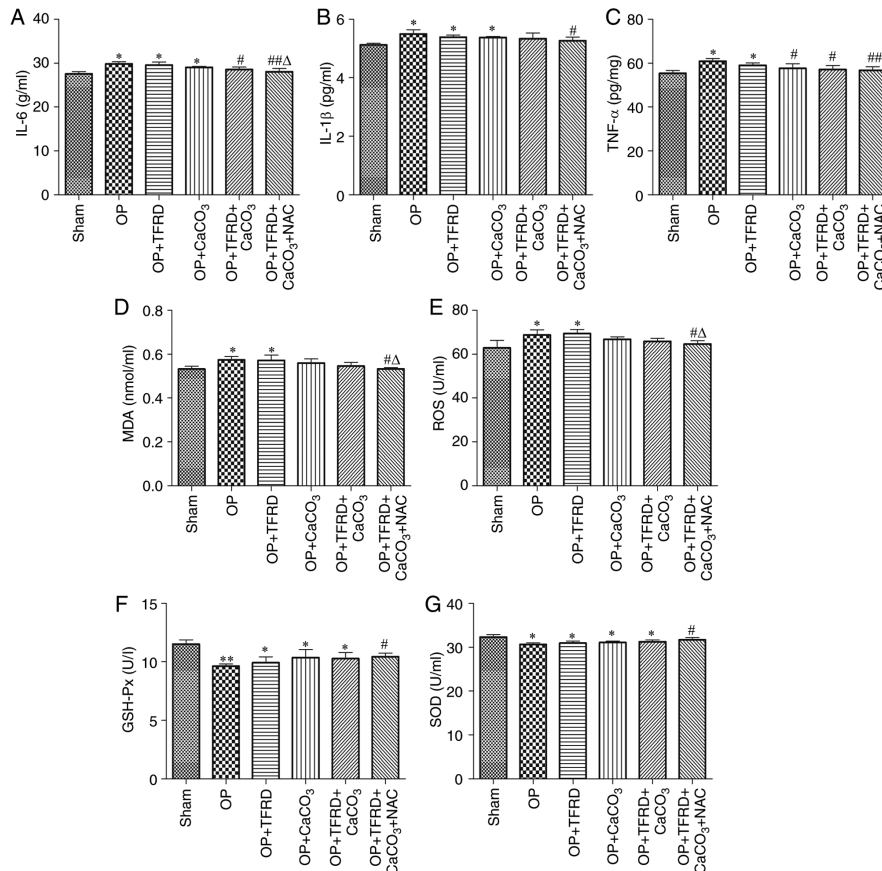


Figure 4. Analysis of inflammatory and oxidative stress-related factors. Serum levels of (A) IL-6; (B) IL-1β; and (C) TNF-α. (D)MDA content. Activity of (E) ROS; (F) GSH-Px; and (G) SOD. The data are expressed as the mean ± SD. Compared with the sham-operated group, *P<0.05 and **P<0.01; compared with the OP group, #P<0.05 and ##P<0.01; compared with the OP + TFRD group, ΔP<0.05. MDA, malonaldehyde; ROS, reactive oxygen species; GSH-Px, glutathione peroxidase; SOD, superoxide dismutase; OP, osteoporosis; TFRD, total flavonoids of *Rhizoma Drynariae*; CaCO₃, calcium carbonate; NAC, N-acetyl cysteine.

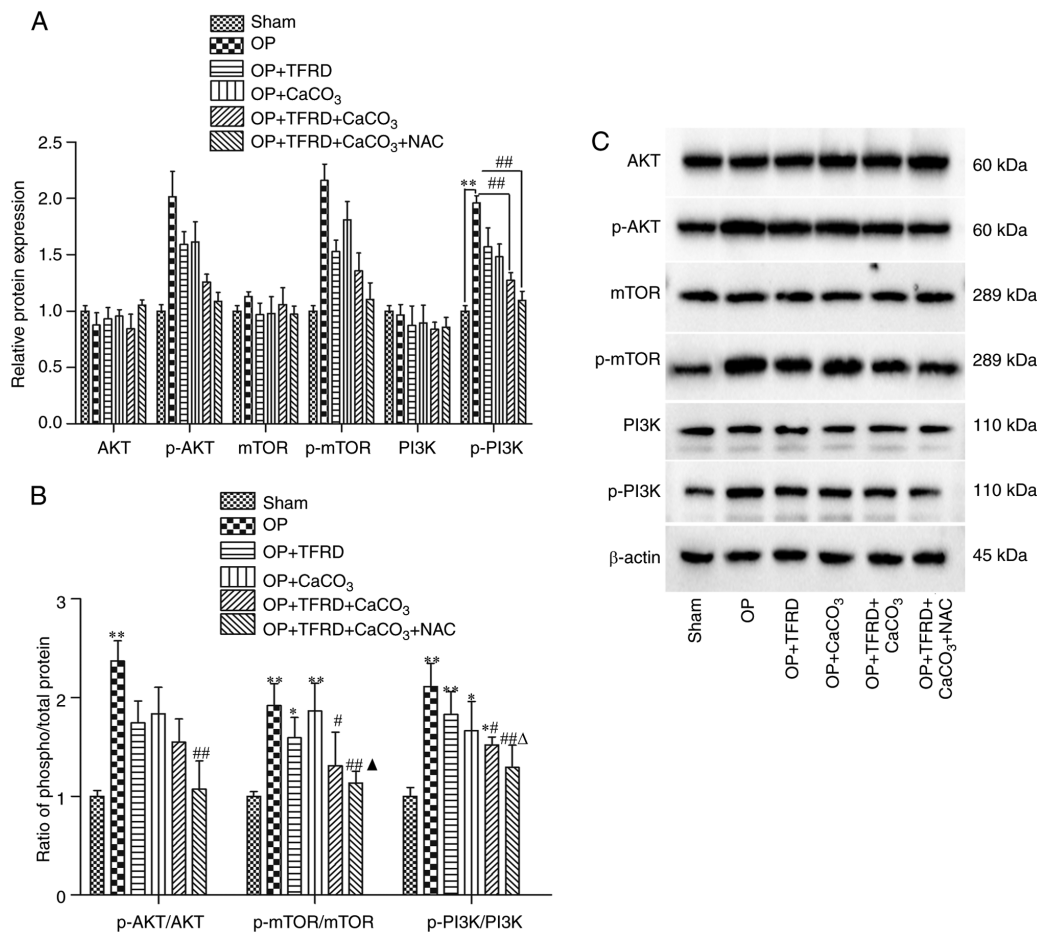


Figure 5. Western blot analysis of oxidative stress pathway-related factors in OP rats. (A) Relative expression of AKT, p-AKT, mTOR, p-mTOR, PI3K and p-PI3K; (B) p-AKT/AKT, p-mTOR/mTOR and p-PI3K/PI3K ratio; (C) Protein band density was calculated as a ratio relative to β -actin protein levels. The data are expressed as the mean \pm SD. Compared with the sham-operated group, * $P < 0.05$ and ** $P < 0.01$; compared with the OP group, # $P < 0.05$ and ## $P < 0.01$; compared with the OP + TFRD group, $\Delta P < 0.05$; compared with the OP + CaCO₃ group, $\blacktriangle P < 0.05$. OP, osteoporosis; TFRD, total flavonoids of *Rhizoma Drynariae*; CaCO₃, calcium carbonate; NAC, N-acetyl cysteine.

$P < 0.01$, $P < 0.05$ and $P < 0.05$, respectively; Fig. 5B). Compared with the OP group, the p-AKT/AKT ratio was significantly decreased in rats of the OP + TFRD + CaCO₃ + NAC group ($P < 0.01$; Fig. 5B), and the p-mTOR/mTOR and p-PI3K/PI3K ratios were markedly decreased in rats of the OP + TFRD + CaCO₃ and OP + TFRD + CaCO₃ + NAC groups ($P < 0.01$ and $P < 0.05$, respectively; Fig. 5B). Compared with the OP + TFRD group, the of p-mTOR/mTOR ratio was significantly decreased in the OP + TFRD + CaCO₃ + NAC group ($P < 0.05$; Fig. 5B). Compared with the OP + CaCO₃ group, the p-PI3K/PI3K ratio was significantly decreased in rats of the OP + TFRD + CaCO₃ + NAC group ($P < 0.05$; Fig. 5B). These results indicated that OP increased the levels of phosphorylated proteins in the oxidative stress pathway, while TFRD, CaCO₃ and NAC supplementation reduced the level of phosphorylated proteins in the oxidative stress pathway in OP rats.

Discussion

The present study reported that TFRD combined with calcium inhibited OP by reducing ROS generation. The results revealed that the supplementation of TFRD, calcium and NAC significantly increased antioxidant capacity, increased BMD and reduced bone mineral loss in rats with OP. These findings

confirmed that TFRD combined with calcium inhibited the occurrence of OP by suppressing ROS generation.

OP is mainly characterized by degenerative changes in bone tissue microstructure, osteopenia and increased bone fragility, thus greatly increasing the risk of fractures (23). Calcium is an important mineral of the body, and the main pathological change of OP is bone mineral loss (15). The decrease of the calcium content leads to an increase in ROS level; by contrast, the addition of antioxidants can significantly restore calcium absorption (24). Therefore, calcium deficiency is an important cause of OP, and calcium supplementation is the most effective and safe method for the prevention and treatment of OP (25). Appropriate calcium supplementation can enhance bone calcium levels and increase bone density, thereby significantly ameliorating bone formation (26). An adequate intake of calcium and vitamin D can prevent bone loss in postmenopausal women and maintain the bone density of the femoral neck and lumbar vertebrae, thus reducing the incidence of fractures (27). The OP rat model is a widely used animal model in the study of OP (28). In the present study, an OP rat model was constructed to evaluate the effects of TFRD combined with calcium on OP. The rats with OP exhibited a severely decreased BMD, BMC, BV/TV and Tb.Th. Treatment with TFRD combined with CaCO₃ significantly increased

bone density and reduced bone mineral loss in OP rats. In addition, the BMD, BMC and BV/TV were normalized in rats with OP following treatment with NAC. These results suggest that NAC enhances the preventive effects of TFRD combined with CaCO₃ on bone loss in OP rats, and this recovery may be mainly achieved through passive calcium absorption.

Accumulating evidence indicates that increased ROS generation and decreased antioxidant defense mechanisms lead to bone loss in OP (29,30). The present study sought to determine whether OP is associated with increased oxidative stress. It has recently been demonstrated that oxidative stress is associated with decreased levels and activity of antioxidant enzymes in mouse vertebral tissue, which leads to decreased osteoblast-mediated bone formation and increased osteoclast-mediated bone resorption (31). The results revealed that the level of ROS and MDA content were significantly increased, and the activity of SOD and the expression of GSH-Px were significantly decreased in rats with OP. TFRD combined with CaCO₃ increased the activities of SOD and GSH-Px, and reduced the production of ROS and MDA in rats with OP, thus exerting antioxidant effects. TFRD and CaCO₃ in combination exerted more prominent effects compared with either treatment alone. Inflammatory factors (such as ILs) are released in patients with OP and it has been demonstrated that they are negatively associated with BMD (32). IL-6 is a multicellular cytokine, and its level changes may reflect the severity of the inflammatory response; under stress conditions, such as infection or tissue injury, the level of serum IL-6 increases (33). IL-1 β and TNF- α can jointly promote the production of other cytokines, such as IL-11 and macrophage colony-stimulating factor, thus promoting the imbalance of bone metabolic coupling (34). In the present study, the results revealed that the expression of IL-6, IL-1 β and TNF- α in OP rats was significantly increased, and the levels of IL-6, IL-1 β and TNF- α were significantly decreased following treatment with TFRD, CaCO₃ and NAC. These results suggested that TFRD, CaCO₃ and NAC treatment improved inflammatory factor levels in rats with OP, and this improvement was at least partly accompanied by changes in the oxidative stress level and inflammatory response.

The increased accumulation of ROS can significantly decrease the expression of the osteogenic marker proteins RUNX2, BGP and OPG (35). RUNX2 is an early marker of osteoblast differentiation, whereas the Wnt pathway and BMP play an osteogenic role by stimulating the expression of RUNX2 (36). Furthermore, high expression of RUNX2 can activate OPN and regulate BGP, while BGP can maintain the normal mineralization rate of bone (37). The regulatory mechanism of osteogenesis and bone resorption was demonstrated by Dufresne *et al.* (38); the process of bone remodeling mainly depends on the expression of OPG and receptor activator of NF- κ B ligand (RANKL) in osteoblasts; OPG blocks the binding of RANKL to RANK and regulates bone resorption by inhibiting osteoclast differentiation (39). The present study demonstrated that the protein expression of RUNX2, OPG and BGP decreased significantly in rats of the OP group. However, the protein expression of RUNX2, OPG and BGP in the OP + TFRD + CaCO₃ and OP + TFRD + CaCO₃ + NAC groups was significantly increased. Adding TFRD to CaCO₃,

following ovariectomy increased RUNX2 expression, while CaCO₃ alone following ovariectomy did not increase RUNX2 expression, which may be due to the fact that TFRD can initiate the differentiation of rat bone marrow mesenchymal cells into osteoblasts and regulate the expression of osteogenic factor mRNA in the Wnt/ β -catenin signaling pathway. In addition, TFRD can also promote the maturation of osteoblasts, thereby stimulating the expression of RUNX2. These results indicated that TFRD, CaCO₃ and NAC supplementation inhibited osteoclast differentiation and prevented the occurrence of OP.

The PI3K/AKT signaling pathway regulates the function of osteoblasts and osteoclasts by affecting their formation, differentiation, proliferation and apoptosis (40). It has been reported that the PI3K/AKT signaling pathway maintains the dynamic balance of bone tissue, not only under normal conditions, but also under pathological conditions (17). It has been demonstrated that RUNX2 can enhance the activity of the PI3K/AKT signaling pathway by upregulating the protein levels of PI3Kp85 subunit, p110 β subunit and AKT (41). At the same time, PI3K/AKT can significantly promote the DNA binding of RUNX2 and RUNX2-dependent transcription (42). When AKT2 is deficient, the gene and protein expression of RUNX2 is low, and the AKT pathway can promote the gene expression of the RUNX2 (43). The feedback regulation between PI3K/AKT and RUNX2 enhances the activity of RUNX2, thus promoting osteogenic differentiations (44). Therefore, the PI3K/AKT pathway is crucial for bone growth and development. In the present study, the results revealed that the PI3K, AKT and mTOR levels in the OP model group exhibited no significant differences from those in the sham operation group; however, the p-PI3K, p-AKT and p-mTOR levels increased significantly, while the p-PI3K, p-AKT, and p-mTOR levels decreased significantly following treatment with TFRD, CaCO₃ and NAC. These results suggested that TFRD, CaCO₃ and NAC supplementation reduced the level of phosphorylated proteins of the oxidative stress pathway in OP rats.

In conclusion, the present study demonstrated that rats with OP exhibited a severely decreased BMD, bone mineral loss, increased oxidative stress and osteogenic marker protein levels; however, treatment with exogenous TFRD and CaCO₃ significantly improved the antioxidant defense, increased BMD and reduced bone mineral loss, thereby preventing or improving OP. The mechanisms of action may be related to the antioxidant properties of these agents.

Acknowledgements

Not applicable.

Funding

The present study was supported by grants from the National Natural Science Foundation of China (grant no. 81403405), the Sichuan Provincial Department of Health (grant no. CKY2014006), the Sichuan Science and Technology Project (grant no. 2019YJ0612) and the Education Department of Sichuan Province (grant no. 14ZB0085).

Availability of materials and data

The datasets used and/or analyzed during the current study are available from the corresponding author on reasonable request.

Authors' contributions

PM and YH conceived and designed the current study. PM, XM, JS, LH and ZZ performed the experiments. PM, XM and JS collected and analyzed the data. PM and YH drafted the manuscript. PM, YH and ZZ revised the manuscript. PM and YH confirm the authenticity of all the raw data. All authors read and approved the final manuscript.

Ethics approval and consent to participate

The present study was approved by the Animal Care Unit and Use Committee of Chengdu University of TCM (approval no.20190078).

Patient consent for publication

Not applicable.

Competing interests

The authors declare that they have no competing interests.

References

- Raisz LG: Pathogenesis of osteoporosis: Concepts, conflicts, and prospects. *J Clin Invest* 115: 3318-3325, 2005.
- Cano A, Chedraui P, Goulis DG, Lopes P, Mishra G, Mueck A, Senturk LM, Simoncini T, Stevenson JC, Stute P, *et al*: Calcium in the prevention of postmenopausal osteoporosis: EMAS clinical guide. *Maturitas* 107: 7-12, 2018.
- Bonaccorsi G, Piva I, Greco P and Cervellati C: Oxidative stress as a possible pathogenic cofactor of post-menopausal osteoporosis: Existing evidence in support of the axis oestrogen deficiency-redox imbalance-bone loss. *Indian J Med Res* 147: 341-351, 2018.
- Zeng Q, Li N, Wang Q, Feng J, Sun D, Zhang Q, Huang J, Wen Q, Hu R, Wang L, *et al*: The Prevalence of Osteoporosis in China, a Nationwide, Multicenter DXA Survey. *J Bone Miner Res* 34: 1789-1797, 2019.
- Omsland TK and Magnus JH: Forecasting the burden of future postmenopausal hip fractures. *Osteoporos Int* 25: 2493-2496, 2014.
- Manolagas SC: From estrogen-centric to aging and oxidative stress: A revised perspective of the pathogenesis of osteoporosis. *Endocr Rev* 31: 266-300, 2010.
- Wang J, Wang G, Gong L, Sun G, Shi B, Bao H and Duan Y: Isoprenaline regulates PPAR γ /WNT to inhibit oxidative stress in osteoporosis. *Mol Med Rep* 17: 1125-1131, 2018.
- An J, Yang H, Zhang Q, Liu C, Zhao J, Zhang L and Chen B: Natural products for treatment of osteoporosis: The effects and mechanisms on promoting osteoblast-mediated bone formation. *Life Sci* 147: 46-58, 2016.
- Shieh P, Jan CR and Liang WZ: The protective effects of the antioxidant N-acetylcysteine (NAC) against oxidative stress-associated apoptosis evoked by the organophosphorus insecticide malathion in normal human astrocytes. *Toxicology* 417: 1-14, 2019.
- Chen L, Wang G, Wang Q, Liu Q, Sun Q and Chen L: N-acetylcysteine prevents orchietomy-induced osteoporosis by inhibiting oxidative stress and osteocyte senescence. *Am J Transl Res* 11: 4337-4347, 2019.
- Raffaele M, Barbagallo I, Licari M, Carota G, Sferrazzo G, Spampinato M, Sorrenti V and Vanella L: N-Acetylcysteine (NAC) ameliorates lipid-related metabolic dysfunction in bone marrow stromal cells-derived adipocytes. *Evid Based Complement Alternat Med* 2018: 5310961, 2018.
- Matera MG, Calzetta L and Cazzola M: Oxidation pathway and exacerbations in COPD: The role of NAC. *Expert Rev Respir Med* 10: 89-97, 2016.
- Gludla PV, Dias SC, Obonye N, Johnson R, Louw J and Nkambule BB: A Systematic Review on the Protective Effect of N-Acetyl Cysteine Against Diabetes-Associated Cardiovascular Complications. *American journal of cardiovascular drugs: drugs, devices, and other interventions* 18: 283-298, 2018.
- Yamada M, Tsukimura N, Ikeda T, Sugita Y, Att W, Kojima N, Kubo K, Ueno T, Sakurai K and Ogawa T: N-acetyl cysteine as an osteogenesis-enhancing molecule for bone regeneration. *Biomaterials* 34: 6147-6156, 2013.
- Sheweta SA and Khoshhal KI: Calcium metabolism and oxidative stress in bone fractures: Role of antioxidants. *Curr Drug Metab* 8: 519-525, 2007.
- Zhou RP, Lin SJ, Wan WB, Zuo HL, Yao FF, Ruan HB, Xu J, Song W, Zhou YC, Wen SY, *et al*: Chlorogenic Acid Prevents Osteoporosis by Shp2/PI3K/Akt Pathway in Ovariectomized Rats. *PLoS One* 11: e0166751, 2016.
- Xi JC, Zang HY, Guo LX, Xue HB, Liu XD, Bai YB and Ma YZ: The PI3K/AKT cell signaling pathway is involved in regulation of osteoporosis. *J Recept Signal Transduct Res* 35: 640-645, 2015.
- Yuan FL, Xu RS, Jiang DL, He XL, Su Q, Jin C and Li X: Leonurine hydrochloride inhibits osteoclastogenesis and prevents osteoporosis associated with estrogen deficiency by inhibiting the NF- κ B and PI3K/Akt signaling pathways. *Bone* 75: 128-137, 2015.
- Wang H, Zhao W, Tian QJ, Xin L, Cui M and Li YK: Effect of lncRNA AK023948 on rats with postmenopausal osteoporosis via PI3K/AKT signaling pathway. *Eur Rev Med Pharmacol Sci* 24: 2181-2188, 2020.
- Song S, Gao Z, Lei X, Niu Y, Zhang Y, Li C, Lu Y, Wang Z and Shang P: Total flavonoids of *Drynariae Rhizoma* prevent bone loss induced by Hindlimb unloading in rats. *Molecules* 22: 22, 2017.
- Fang J, Yang L, Shen JZ, *et al*: Effects of total flavonoids of *Rhizoma Drynariae* on glutamate signal Glu, mGluR5 and EAAT1 in bone of ovariectomized rats. *Chin J Biochem Drugs* 34: 10-12, 16, 2014.
- Zhu F, Liu Z and Ren Y: Mechanism of melatonin combined with calcium carbonate on improving osteoporosis in aged rats. *Exp Ther Med* 16: 192-196, 2018.
- Ensrud KE and Crandall CJ: Osteoporosis. *Ann Intern Med* 167: ITC17-ITC32, 2017.
- Bidwell JP, Alvarez MB, Hood M Jr and Childress P: Functional impairment of bone formation in the pathogenesis of osteoporosis: The bone marrow regenerative competence. *Curr Osteoporos Rep* 11: 117-125, 2013.
- Weaver CM, Alexander DD, Boushey CJ, Dawson-Hughes B, Lappe JM, LeBoff MS, Liu S, Looker AC, Wallace TC and Wang DD: Calcium plus vitamin D supplementation and risk of fractures: an updated meta-analysis from the National Osteoporosis Foundation. *Osteoporos Int* 27: 367-376, 2016.
- Shuid AN, Mohamad S, Mohamed N, Fadzilah FM, Mokhtar SA, Abdullah S, Othman F, Suhaimi F, Muhammad N and Soelaiman IN: Effects of calcium supplements on fracture healing in a rat osteoporotic model. *Orthop Res* 28: 1651-1656, 2010.
- Paschalis EP, Gamsjaeger S, Hassler N, Fahrleitner-Pammer A, Dobnig H, Stepan JJ, Pavo I, Eriksen EF and Klaushofer K: Vitamin D and calcium supplementation for three years in postmenopausal osteoporosis significantly alters bone mineral and organic matrix quality. *Bone* 95: 41-46, 2017.
- Zhang F, Xie J, Wang G, Zhang G and Yang H: Anti-osteoporosis activity of Sanguinarine in preosteoblast MC3T3-E1 cells and an ovariectomized rat model. *J Cell Physiol* 233: 4626-4633, 2018.
- Cervellati C, Bonaccorsi G, Cremonini E, Bergamini CM, Patella A, Castaldini C, Ferrazzini S, Capatti A, Picarelli V, Pansini FS, *et al*: Bone mass density selectively correlates with serum markers of oxidative damage in post-menopausal women. *Clin Chem Lab Med* 51: 333-338, 2013.
- Cervellati C and Bergamini CM: Oxidative damage and the pathogenesis of menopause related disturbances and diseases. *Clin Chem Lab Med* 54: 739-753, 2016.
- Wu X, Li J, Zhang H, Wang H, Yin G and Miao D: Pyrroloquinoline quinone prevents testosterone deficiency-induced osteoporosis by stimulating osteoblastic bone formation and inhibiting osteoclastic bone resorption. *Am J Transl Res* 9: 1230-1242, 2017.

32. Orchard T, Yildiz V, Steck SE, Hébert JR, Ma Y, Cauley JA, Li W, Mossavar-Rahmani Y, Johnson KC, Sattari M, *et al*: Dietary inflammatory index, bone mineral density, and risk of fracture in postmenopausal women: Results from the Women's Health Initiative. *J Bone Miner Res* 32: 1136-1146, 2017.
33. Chen B and Li HZ: Association of IL-6 174G/C (rs1800795) and 572C/G (rs1800796) polymorphisms with risk of osteoporosis: A meta-analysis. *BMC Musculoskelet Disord* 21: 330, 2020.
34. Al-Daghri NM, Aziz I, Yakout S, Aljohani NJ, Al-Saleh Y, Amer OE, Sheshah E, Younis GZ and Al-Badr FBM: Inflammation as a contributing factor among postmenopausal Saudi women with osteoporosis. *Medicine (Baltimore)* 96: e5780, 2017.
35. Wang Q, Li Y, Zhang Y, Ma L, Lin L, Meng J, Jiang L, Wang L, Zhou P and Zhang Y: lncRNA MEG3 inhibited osteogenic differentiation of bone marrow mesenchymal stem cells from postmenopausal osteoporosis by targeting miR-133a-3p. *Biomed Pharmacother* 89: 1178-1186, 2017.
36. Zhu W, He X, Hua Y, Li Q, Wang J and Gan X: The E3 ubiquitin ligase WWP2 facilitates RUNX2 protein transactivation in a mono-ubiquitination manner during osteogenic differentiation. *J Biol Chem* 292: 11178-11188, 2017.
37. Zhu XB, Lin WJ, Lv C, Wang L, Huang ZX, Yang SW and Chen X: MicroRNA-539 promotes osteoblast proliferation and differentiation and osteoclast apoptosis through the AXNA-dependent Wnt signaling pathway in osteoporotic rats. *J Cell Biochem* 119: 8346-8358, 2018.
38. Dufresne SS, Dumont NA, Bouchard P, Lavergne É, Penninger JM and Frenette J: Osteoprotegerin protects against muscular dystrophy. *Am J Pathol* 185: 920-926, 2015.
39. Wolski H, Drews K, Bogacz A, Kamiński A, Barlik M, Bartkowiak-Wieczorek J, Klejewski A, Ożarowski M, Majchrzycki M and Seremak-Mrozikiewicz A: The RANKL/RANK/OPG signal trail: Significance of genetic polymorphisms in the etiology of postmenopausal osteoporosis. *Ginekol Pol* 87: 347-352, 2016.
40. Mukherjee A and Rotwein P: Selective signaling by Akt1 controls osteoblast differentiation and osteoblast-mediated osteoclast development. *Mol Cell Biol* 32: 490-500, 2012.
41. Ouyang N, Zhang P, Fu R, Shen G, Jiang L and Fang B: Mechanical strain promotes osteogenic differentiation of bone mesenchymal stem cells from ovariectomized rats via the phosphoinositide 3 kinase/Akt signaling pathway. *Mol Med Rep* 17: 1855-1862, 2018.
42. Kita K, Kimura T, Nakamura N, Yoshikawa H and Nakano T: PI3K/Akt signaling as a key regulatory pathway for chondrocyte terminal differentiation. *Genes to cells: Devoted to molecular & cellular mechanisms* 13: 839-850, 2008.
43. Li M, Luo R, Yang W, Zhou Z and Li C: miR-363-3p is activated by MYB and regulates osteoporosis pathogenesis via PTEN/PI3K/AKT signaling pathway. *In Vitro Cell Dev Biol Anim* 55: 376-386, 2019.
44. Zhang Y, Cao X, Li P, Fan Y, Zhang L, Li W and Liu Y: PSMC6 promotes osteoblast apoptosis through inhibiting PI3K/AKT signaling pathway activation in ovariectomy-induced osteoporosis mouse model. *J Cell Physiol* 235: 5511-5524, 2020



This work is licensed under a Creative Commons Attribution-NonCommercial-NoDerivatives 4.0 International (CC BY-NC-ND 4.0) License.